

# Tuning Photophysical and Electrochemical Properties of Phosphorescent Heteroleptic Iridium Complex Salts—as Chemosensors

J. Jayabharathi · R. Sathishkumar · V. Thanikachalam · K. Jayamoorthy

Received: 27 August 2013 / Accepted: 27 September 2013 / Published online: 11 October 2013  
© Springer Science+Business Media New York 2013

**Abstract** Photophysical and electrochemical studies of cyclometalated cationic heteroleptic iridium(III) complex salts have been carried out. For these complex salts the intense absorption bands appeared around 263 nm and are assigned to spin-allowed  $\pi$ - $\pi^*$  transitions of phenanthroline ligands. Moderately intense and weak absorption bands observed around 341 and 440 nm, respectively. These bands are assigned to spin-allowed metal to ligand charge transfer  $^1\text{MLCT}$  and  $^3\text{MLCT}$  transitions, respectively. The influence of anions and proton on the photophysical and electrochemical studies were also carried out. The emission wavelength was red shifted and emission color changed from yellow to red by the addition of  $\text{CF}_3\text{CO}_2\text{H}$ . The solution color changed from green to brown and the emission was quenched by the addition anions such as of  $\text{F}^-$ ,  $\text{CH}_3\text{COO}^-$  and  $\text{H}_2\text{PO}_4^-$ .

**Keywords** Iridium complex salt · Green emitter · Photoluminescence

## Introduction

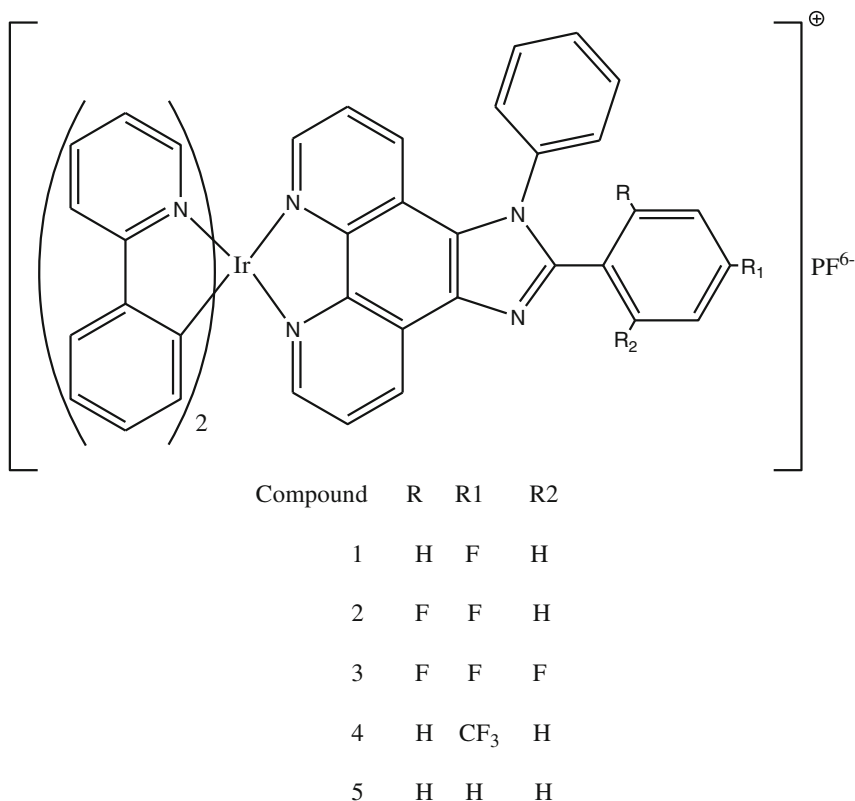
Phosphorescent transition-metal complexes have drawn great attention in research and industry because of their excellent performance when used as colorful emitters in organic light emitting diodes (OLEDs). Among them, cyclometalated iridium(III) complexes are regarded as the most successful phosphorescent material [1, 2] owing to their high photoluminescence efficiency, relatively short lifetime and flexible

color tunability [3–8]. Many phosphorescent heavy-metal complexes, such as platinum(II), rhenium(I) and ruthenium(II) complexes, have been explored as chemosensors for anions [9], oxygen concentration [10] and metal ions [11]. However, as the best phosphorescent dyes [12, 13], the application of iridium(III) complexes in chemosensors were mainly limited to recognizing oxygen [14, 15] and the  $\text{Hg}^{2+}$  cation [16]. Anion recognition and sensing have been of most interest in recent years because of their important role in biological processes and environmental assays [17–19]. Various types of pure organic dyes have been used as receptors for anionic species [17–27]. Although iridium(III) complex salts has been reported to recognize a few anions and protons [28–30], introduction of electron withdrawing substituent tunes the emission and absorption. Sensitivity to proton and anion might be expected for iridium(III) complexes incorporating an imidazo[4,5-*f*][1, 10]-phenanthroline unit. Herein, four cationic iridium(III) complex salts  $[\text{Ir}(\text{ppy})_2(\text{N}^{\wedge}\text{N})]^+\text{PF}_6^-$  based on different phenanthroline derivatives ( $\text{N}^{\wedge}\text{N}$  ligands) with highly electron withdrawing fluoro- and trifluoromethyl- substituents at desired positions were synthesized and tuning of their photophysical and electrochemical properties by anions and proton was investigated.

## Experimental

The ultraviolet–visible (UV–vis) spectra of the phosphorescent iridium complex salts were measured in an UV–vis spectrophotometer (Perkin Elmer Lambda 35) and corrected for background absorption due to solvent. Photoluminescence (PL) spectra were recorded on a (Perkin Elmer LS55) fluorescence spectrometer. NMR spectra were recorded on Bruker 400 MHz NMR spectrometer. The mass spectra of the samples were obtained using a Agilent LCMS VL SD in electron ionization mode. Cyclic voltammetry (CV) analysis were

J. Jayabharathi (✉) · R. Sathishkumar · V. Thanikachalam · K. Jayamoorthy  
Department of Chemistry, Annamalai University,  
Annamalainagar 608 002, Tamilnadu, India  
e-mail: jtchalam2005@yahoo.co.in

**Chart 1** Chemical structures of complex salts 1–5

performed by using CHI 630A potentiostat electrochemical analyzer. Measurements of oxidation and reduction were undertaken using 0.1 M tetra(n-butyl)ammonium- hexafluorophosphate as the supporting electrolyte, at scan rate of 0.1 V S<sup>-1</sup>. The potentials were measured against an Ag/Ag<sup>+</sup> (0.01 M AgNO<sub>3</sub>) reference electrode using ferrocene/ferrocenium (CP<sub>2</sub>Fe/CP<sub>2</sub>Fe<sup>+</sup>) as the internal standard. The onset potentials were determined from the intersection of two tangents drawn at the rising current and background current of the cyclic voltammogram. Fluorescence lifetime measurements were carried out with a nanosecond time correlated single photon counting (TCSPC) spectrometer Horiba Fluorocube-01-NL lifetime system with NanoLED (pulsed diode exCitation source) as the excitation source and TBX-PS as detector. The slit width was 8 nm and the excitation wavelength was 282 nm. The time correlated single photon counting (TCSPC) results fit to single exponential decay, DAS6 software was used for the fit and the  $\chi^2$  values are less than 1.2 and not less than 1. The lifetime measurements of all iridium(III) complex salts were made and the signal was measured at the emission wavelength of individual compound. The absolute PL quantum yields were measured by comparing fluorescence intensities (integrated areas) of a standard sample (Coumarin 46) and the unknown sample using the formula  $\Phi_{\text{unk}} = \Phi_{\text{std}} \left( \frac{I_{\text{unk}}}{I_{\text{std}}} \right) \left( \frac{A_{\text{std}}}{A_{\text{unk}}} \right) \left( \frac{n_{\text{unk}}}{n_{\text{std}}} \right)^2$  where,  $\Phi_{\text{unk}}$  is the fluorescence quantum yield of the sample,  $\Phi_{\text{std}}$  is the fluorescence quantum yield of the standard;  $I_{\text{unk}}$  and  $I_{\text{std}}$

are the integrated emission intensities of the sample and the standard, respectively.  $A_{\text{unk}}$ , and  $A_{\text{std}}$  are the absorbance of the sample and the standard at the excitation wavelength, respectively.  $n_{\text{unk}}$  and  $n_{\text{std}}$  are the indexes of refraction of the sample and standard solutions.

#### Synthesis of Phenanthroline Derivatives

The phenanthroline derivatives were synthesized according to our previous report [31].

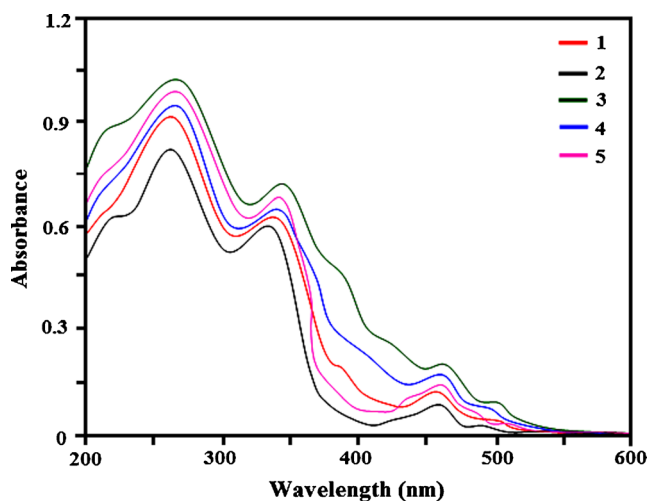


**Fig. 1** Absorption spectra of the iridium complex salts 1–5 ( $10^{-4}$  M) in CH<sub>2</sub>Cl<sub>2</sub>

**Table 1** Absorption ( $\lambda_{\text{abs}}$ , nm), fluorescence quantum yield ( $\Phi$ ), lifetime ( $\tau$ ,  $\mu\text{s}$ ), radiative rate constant ( $k_r$ ,  $\text{s}^{-1}$ ), nonradiative rate constant ( $k_{\text{nr}}$ ,  $\text{s}^{-1}$ ) and electrochemical behavior of **1–5**

Complex salts	$\lambda_{\text{abs}}$	$\Phi$	$\tau$	$k_r$	$k_{\text{nr}}$	$E^{\text{ox}}/V$	$E^{\text{re}}/V$
1	263, 342, 460, 482	0.25	0.82	0.30	0.92	1.05	-1.97
2	264, 341, 456, 478	0.24	0.71	0.34	1.06	1.08	-2.02
3	265, 342, 464, 483	0.28	0.69	0.41	1.03	1.10	-2.04
4	267, 342, 449, 485	0.28	0.70	0.37	1.05	1.09	-2.03
5	266, 341, 451, 480	0.26	0.73	0.36	1.01	1.07	-1.99

### Synthesis of Iridium(III)Complex Salts

The cyclometalated iridium(III) chlorobridged dimer  $[\text{Ir}(\text{ppy})_2\text{Cl}]_2$  was prepared according to literature methods [32]. A solution of  $[\text{Ir}(\text{ppy})_2\text{Cl}]_2$  (0.079 mmol) and 2-(4-fluorophenyl)-1-phenyl-1H-imidazo[4,5-f][1, 10]phenanthroline [FPIP] (0.172 mmol) in dichloromethane-ethanol (30 mL, 2:1 v/v) have been refluxed for 6 h. To the yellow solution, 12-fold excess of potassium hexafluorophosphate has been added. The colloidal solution was stirred for 4 h and filtered to remove insoluble inorganic salts. The yellow solid was washed with dichloromethane-acetone.

#### Complex Salt 1: $\text{Ir}[(\text{fppi}) (\text{ppy})_2]$

Yield: 65 %. Anal. Calcd. for  $\text{C}_{41}\text{H}_{27}\text{F}_7\text{IrN}_6\text{P}$ : C, 52.78; H, 3.40; N, 8.21. Found: C, 83.61; H, 4.32; N, 7.30.  $^1\text{H}$  NMR (400 MHz,  $d_6$ -DMSO):  $\delta$  9.08 (d, 2H,  $J=8.8$ ), 8.19 (t, 4H,  $J=7.6$ ), 8.11 (d, 2H,  $J=5.2$ ), 8.01–8.06 (m, 2H), 7.89 (d, 2H,  $J=8.4$ ), 7.74 (t, 2H,  $J=7.6$ ), 7.58 (t, 2H,  $J=7.2$ ), 7.52 (t, 1H,  $J=7.8$ ), 7.47 (d, 2H,  $J=6.4$ ), 7.02 (d, 2H,  $J=6.8$ ), 6.88–6.96 (m, 3H), 6.24 (d, 2H,  $J=7.6$ ).  $^{13}\text{C}$  NMR (100 MHz,  $d_6$ -DMSO):  $\delta$  113.25, 115.76, 118.61, 120.98, 122.55, 123.14, 123.45, 124.17, 125.22, 125.77, 126.38, 126.70, 126.88, 127.23, 127.48, 127.90, 128.36, 129.31, 130.04, 130.49, 131.35, 131.73, 135.50, 136.81, 147.97, 160.54, 162.08. MS: m/z. 815.13  $[\text{M-PF}_6]$ .

#### Complex Salt 2: $\text{Ir}[(\text{dfppi}) (\text{ppy})_2]$

Yield: 65 %. Anal. Calcd. for  $\text{C}_{41}\text{H}_{26}\text{F}_8\text{IrN}_6\text{P}$ : C, 53.24; H, 2.61; N, 7.01. Found: C, 53.55; H, 2.82; N, 7.15.  $^1\text{H}$  NMR (400 MHz,

$d_6$ -DMSO):  $\delta$  9.12 (d, 2H,  $J=8.0$ ), 8.23 (t, 3H,  $J=7.6$ ), 8.18 (d, 2H,  $J=5.2$ ), 8.05–8.11 (m, 1H), 7.82 (d, 2H,  $J=8.0$ ), 7.69 (t, 2H,  $J=6.4$ ), 7.54 (t, 2H,  $J=7.2$ ), 7.41 (t, 1H,  $J=7.6$ ), 7.02 (d, 2H,  $J=7.2$ ), 6.82–6.91 (m, 2H), 6.20 (d, 2H,  $J=7.2$ ).  $^{13}\text{C}$  NMR (100 MHz,  $d_6$ -DMSO):  $\delta$  115.34, 115.46, 119.31, 121.58, 122.65, 123.24, 123.48, 124.26, 125.14, 125.68, 126.42, 126.69, 126.91, 127.33, 127.58, 127.70, 128.44, 129.25, 130.14, 130.56, 131.29, 131.89, 136.58, 137.85, 149.48, 161.11, 163.28. MS: m/z. 833.56  $[\text{M-PF}_6]$ .

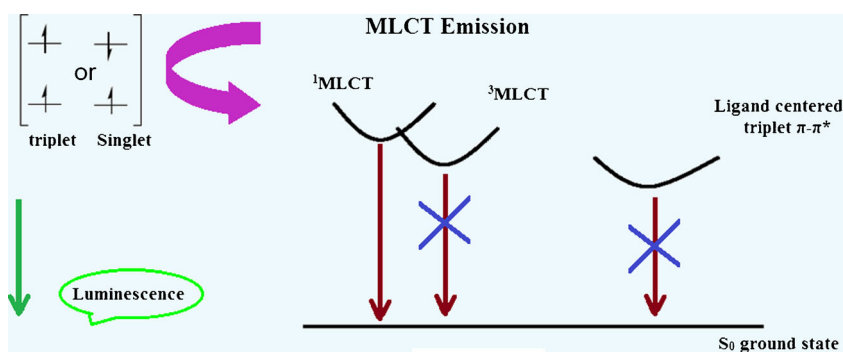
#### Complex Salt 3: $\text{Ir}[(\text{fppi}) (\text{ppy})_2]$

Yield: 60 %. Anal. Calcd. for  $\text{C}_{41}\text{H}_{25}\text{F}_9\text{IrN}_6\text{P}$ : C, 50.76; H, 4.20; N, 8.13. Found: C, 50.91; H, 4.41; N, 8.30.  $^1\text{H}$  NMR (400 MHz,  $d_6$ -DMSO):  $\delta$  9.02 (d, 2H,  $J=8.4$ ), 8.22 (t, 2H,  $J=7.2$ ), 8.12 (d, 2H,  $J=6.0$ ), 8.00–8.04 (m, 2H), 7.74 (d, 2H,  $J=8.2$ ), 7.65 (t, 2H,  $J=7.8$ ), 7.52 (t, 2H,  $J=7.6$ ), 7.43 (d, 2H,  $J=7.2$ ), 6.95 (d, 2H,  $J=6.4$ ), 6.84–6.93 (m, 2H), 6.31 (d, 2H,  $J=7.2$ ).  $^{13}\text{C}$  NMR (100 MHz,  $d_6$ -DMSO):  $\delta$  114.97, 115.44, 117.21, 120.23, 121.05, 123.08, 123.51, 124.34, 125.09, 125.57, 126.24, 126.53, 126.98, 127.25, 127.54, 127.87, 128.39, 129.04, 130.28, 130.85, 131.33, 131.76, 136.62, 137.54, 149.55, 162.58, 163.89. MS: m/z. 851.52  $[\text{M-PF}_6]$ .

#### Complex Salt 4: $\text{Ir}[(\text{fmpipi}) (\text{ppy})_2]$

Yield: 62 %. Anal. Calcd. for  $\text{C}_{42}\text{H}_{27}\text{F}_9\text{IrN}_6\text{P}$ : C, 51.98; H, 4.16; N, 8.31. Found: C, 52.11; H, 4.37; N, 8.47.  $^1\text{H}$  NMR (400 MHz,  $d_6$ -DMSO):  $\delta$  9.12 (d, 2H,  $J=8.2$ ), 8.15 (d, 2H,  $J=6.0$ ), 7.98–8.03 (m, 2H), 7.83 (d, 2H,  $J=8.0$ ), 7.71 (t, 1H,  $J=7.8$ ), 7.51 (t, 2H,  $J=8.2$ ), 7.46 (t, 1H,  $J=7.2$ ), 7.31 (d, 2H,  $J=6.0$ ), 7.05 (d, 2H,  $J=6.4$ ), 6.75–6.86 (m, 4H), 6.13 (d, 2H,

**Fig. 2** Spin-orbit coupling of heavy-metal facilitated triplet emission



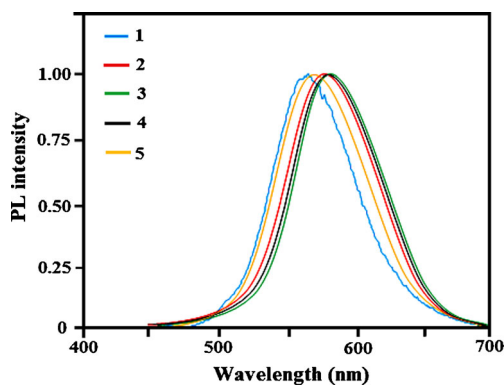


**Fig. 3** Photoluminescent spectra of the iridium complex salt **1** ( $10^{-5}$  M) in  $\text{CH}_2\text{Cl}_2$ ,  $\text{CH}_3\text{CN}$  and solid film

$J=7.2$ ).  $^{13}\text{C}$  NMR (100 MHz,  $d_6$ -DMSO):  $\delta$  114.65, 115.35 117.24, 120.67, 121.48, 122.14, 123.37, 124.85, 125.27, 125.59, 126.35, 126.71, 126.94, 127.23, 127.73, 127.89, 128.36, 129.68, 130.23, 130.65, 131.43, 131.97, 135.28, 136.75, 147.44, 160.17, 162.50. MS:  $m/z$ . 865.58 [ $\text{M-PF}_6$ ].

#### Complex Salt 5: $\text{Ir}[(ppi)(ppy)_2]$

Yield: 62 %. Anal. Calcd. for  $\text{C}_{47}\text{H}_{32}\text{F}_7\text{IrN}_6\text{P}$ : C, 50.45; H, 3.56; N, 7.65. Found: C, 50.31; H, 3.47; N, 7.57.  $^1\text{H}$  NMR (400 MHz,  $d_6$ -DMSO):  $\delta$  8.87 (d, 2H,  $J=7.8$ ), 8.14 (d, 2H,  $J=6.0$ ), 8.04–8.09 (m, 4H), 7.79 (d, 2H,  $J=8.2$ ), 7.67 (t, 2H,  $J=8.2$ ), 7.49 (t, 3H,  $J=6.2$ ), 7.33 (t, 1H,  $J=7.8$ ), 7.29 (d, 2H,  $J=7.4$ ), 7.07 (d, 2H,  $J=6.8$ ), 6.75–6.83 (m, 3H), 6.34 (d, 2H,  $J=6.8$ ).  $^{13}\text{C}$  NMR (100 MHz,  $d_6$ -DMSO):  $\delta$  113.23, 115.64 116.84, 119.61, 121.25, 122.54, 123.41, 124.69, 125.01, 125.64, 126.44, 126.88, 126.97, 127.14, 127.58, 127.91, 128.29, 129.71, 130.24, 130.59, 131.36, 131.89, 135.32, 136.69, 147.28, 161.24, 161.47. MS:  $m/z$ . 892.62 [ $\text{M-PF}_6$ ] Chart 1.

## Results and Discussion

### Absorption and Photoluminescence (PL) Spectra

The absorption spectrum of the complex salts **1–5** in dichloromethane at room temperature shown in Fig. 1. The absorption bands of iridium(III) complex salts show three kinds of bands (Table 1). The intense band observed around 263 nm can be assigned to the allowed ligand centered ( $\pi$ - $\pi^*$ )

**Table 2** Photoluminescent data ( $\lambda_{\text{emi}}$ , nm) of **1–5**

( $\lambda_{\text{emi}}$ , nm)	1	2	3	4	5
$\text{CH}_2\text{Cl}_2$	564	578	582	580	566
$\text{CH}_3\text{CN}$	572	589	598	594	578
Solid film	565	577	584	581	568

transitions [33] and somewhat weaker bands also observed in the lower part of energy. The band position, size and extinction coefficient of the bands observed in the range 341–485 nm suggest that these are MLCT transitions ( $^1\text{MLCT}$  and  $^3\text{MLCT}$ ) [34, 35]. Similar to our earlier reports [36–38], weak bands located at longer wavelength have been assigned

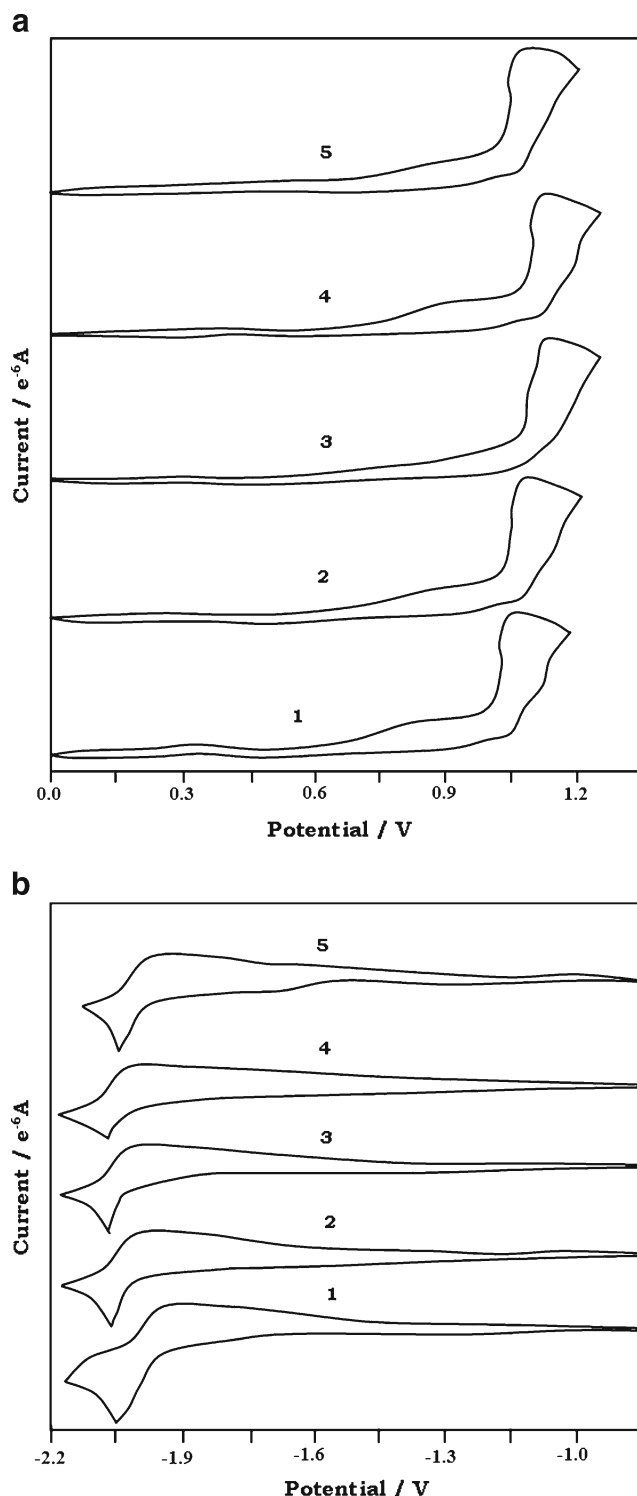


**Fig. 4** Cyclic voltammogram of complex salts **1–5**

to the  $^1\text{MLCT} \leftarrow \text{S}_0$  and  $^3\text{MLCT} \leftarrow \text{S}_0$  transitions of cationic iridium complexes. The intensity of the  $^3\text{MLCT} \leftarrow \text{S}_0$  transition is close to that of  $^1\text{MLCT} \leftarrow \text{S}_0$  transition, suggesting that  $^3\text{MLCT} \leftarrow \text{S}_0$  transition is strongly allowed by S-T mixing of spin-orbit coupling [39]. Absorption around 460 nm for complex salts corresponds to the transition of the  $^1\text{MLCT}$  state as evident from its extinction coefficient of the order  $10^3$ . The absorption like long tail toward lower energy and higher wavelength around 478 nm is assigned to  $^3\text{MLCT}$  transition and gains intensity by mixing with the higher lying  $^1\text{MLCT}$

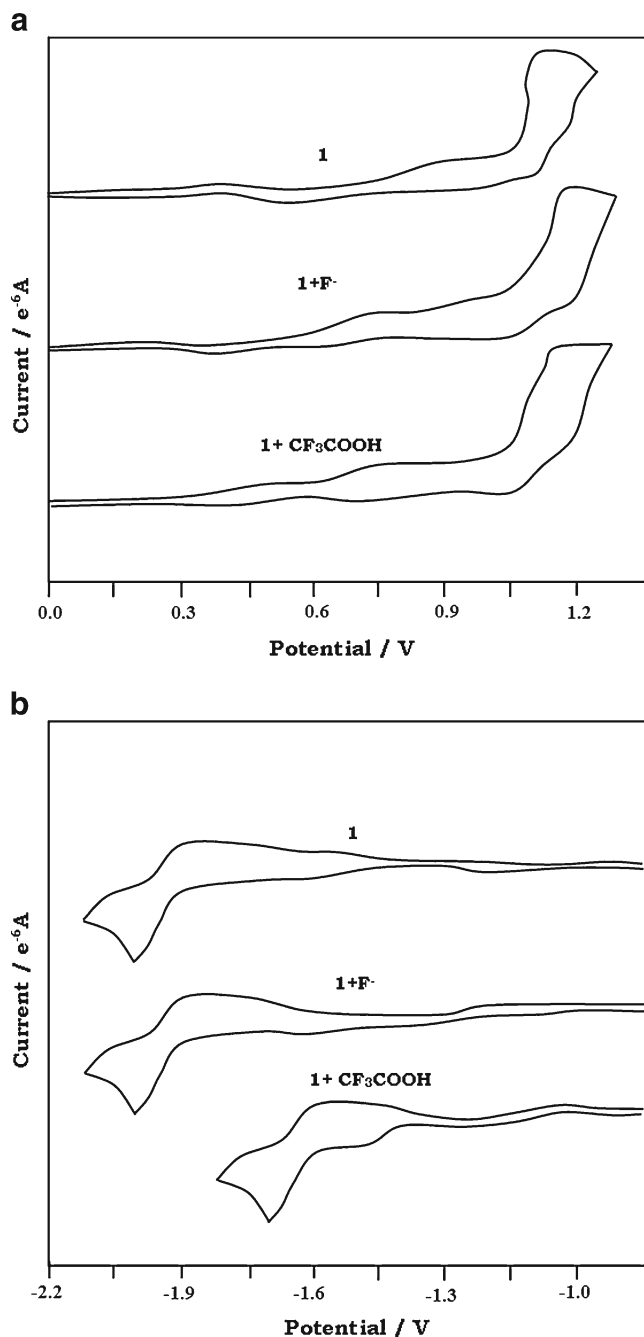


**Fig. 5** Cyclic voltammogram of **1** before and after addition of F<sup>-</sup> and CF<sub>3</sub>COOH

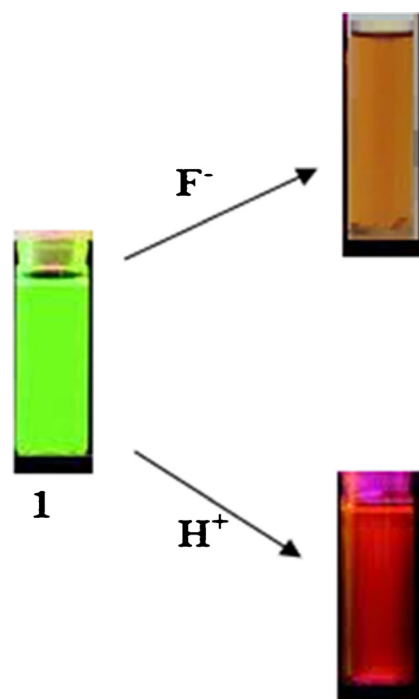


**Fig. 6** Color and emission color variations observed in acetonitrile solutions of **1** ( $5 \times 10^{-4}$  M) in the presence of 2 equiv of F<sup>-</sup> and CF<sub>3</sub>COOH

transition through the spin-orbit coupling of iridium(III) complex salts shown in Fig. 2 [40]. Both singlet MLCT ( $^1\text{MLCT}$ ) and triplet MLCT ( $^3\text{MLCT}$ ) bands are typically observed for these cationic complexes in all solvents. In order for these iridium(III) complexes to be useful as phosphors strong spin-orbit coupling must be present to efficiently mix the singlet and triplet excited states.

The room-temperature photoluminescence spectra of all complex salts in CH<sub>2</sub>Cl<sub>2</sub> solution are shown in Fig. 3 and corresponding photoluminescence data of all complex salts are summarized in Table 2. All complex salts emit intense luminescence with emission wavelengths in the range 564–582 nm in CH<sub>2</sub>Cl<sub>2</sub> solution. The observed emission lifetimes in the microsecond time scales indicate the phosphorescent nature of the emissions. In addition, photoluminescence spectra of these complex salts in solid film were also measured and are similar to those in CH<sub>2</sub>Cl<sub>2</sub> solution. The emission maxima for all complex salts occur at higher energy in less polar CH<sub>2</sub>Cl<sub>2</sub> than those in more polar CH<sub>3</sub>CN, which is very common for cyclometalated iridium(III) diimine MLCT emitters [16].

**Table 3** Binding constants (*K*) of complex salts 1–4

Anions	1	2	3	4
F <sup>-</sup>	$6.98 \times 10^4$	$8.62 \times 10^4$	$9.98 \times 10^4$	$8.85 \times 10^4$
CH <sub>3</sub> COO <sup>-</sup>	$2.63 \times 10^4$	$2.03 \times 10^4$	$3.61 \times 10^4$	$2.45 \times 10^4$
H <sub>2</sub> PO <sub>4</sub> <sup>-</sup>	$4.92 \times 10^3$	$3.82 \times 10^3$	$4.01 \times 10^3$	$3.98 \times 10^3$

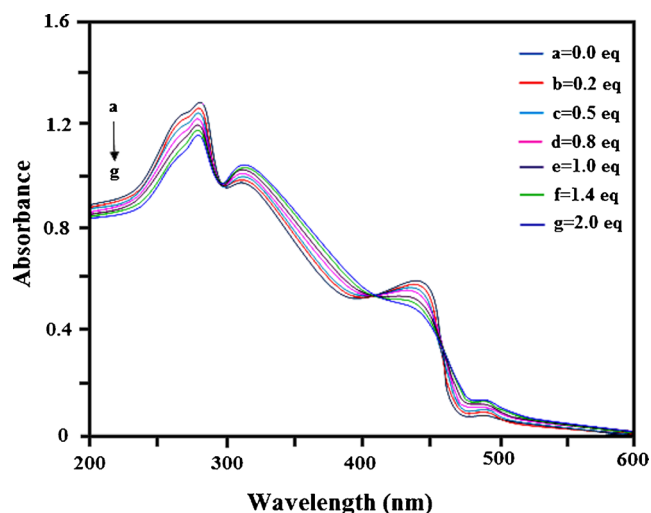


**Fig. 7** Changes in the UV-vis absorption spectra of **1–5** ( $10^{-4}$  M) in  $\text{CH}_3\text{CN}$  solution with various amounts of  $\text{F}^-$  (a to g=0.00 equiv to 2.00 equiv)

### Mixing of Excited States (LC and MLCT)

In the present study the lowest excited state was assigned to  $^3\text{MLCT}$ . Short lifetime, broad luminescence spectra and absorption peaks of those complexes show clearly that the lowest triplet states of those complexes are predominantly  $^3\text{MLCT}$ . For more detail, we should consider degree of mixing to understand the photochemical differences of those complexes according to Eq. 1,

$$\Phi_{\text{T}} = a\Phi_{\text{T}}(\pi-\pi^*) + b\Phi_{\text{T}}(\text{MLCT}) \quad (1)$$

where ‘ $a$ ’ and ‘ $b$ ’ are the normalized co-efficient,  $\Phi_{\text{T}}(\pi-\pi^*)$  and  $\Phi_{\text{T}}(\text{MLCT})$  are the wave function of  $^3(\pi-\pi^*)$  and  $^3(\text{MLCT})$  excited states, respectively. For these iridium complexes, the wave function of the triplet state ( $\Phi_{\text{T}}$ ) responsible for the phosphorescence and equation (1) implies that the excited triplet state of these iridium complexes are mixture

of  $\Phi_{\text{T}}(\pi-\pi^*)$  and  $\Phi_{\text{T}}(\text{MLCT})$  [41]. The triplet state is attributed to dominantly  $^3\pi-\pi^*$  excited state when  $a > b$  and dominantly  $^3\text{MLCT}$  excited state when  $b > a$  [42, 43].

The fluorescence spectra (Fig. 3) of these complex salts **1–5** obtained at 298 K show significant broad shape. According to our previous studies [35–38], phosphorescence spectra from the ligand centered  $^3\pi-\pi^*$  state display vibronic progressions, while those from the  $^3\text{MLCT}$  state [44, 45] are broad in shape. Iridium complex salts **2**, **3** and **4** have excited state with large contribution of  $^3\text{MLCT}$  whereas **1** has excited state with large contribution of  $^3\pi-\pi^*$  [46, 47]. These complex salts are having appreciable quantum yield ( $\Phi$ ). By using  $\Phi$  and life time, the  $k_{\text{r}}$  and  $k_{\text{nr}}$  values are calculated which are displayed in Table 1.

### Electrochemical Properties

The electrochemical properties of the complex salts were studied by cyclic voltammetry (Fig. 4a&b) and the data are listed in Table 1. An irreversible oxidation wave was observed at similar potentials between 1.05 and 1.10 V for all complex salts. It is assumed that pure metal-centered oxidation is reversible and irreversibility increases as the contribution to the HOMO of the cyclometalating phenyl group increases [48]. Therefore, the irreversible oxidation process is assigned to orbits receiving a strong contribution from the iridium center and Ir-C- $\sigma$ -bond orbits at the same time. All complex salts exhibit a similar irreversible reduction wave at approximately  $-2.00$  V. This reduction wave of **1–5** can be assigned to the reduction of the phenanthroline ligands.

### Effect Anions on Tuning Photophysical and Electrochemical Properties

The complexation abilities of **1–4** with anions were investigated by UV-vis absorption titration experiments (Fig. 5a&b). By

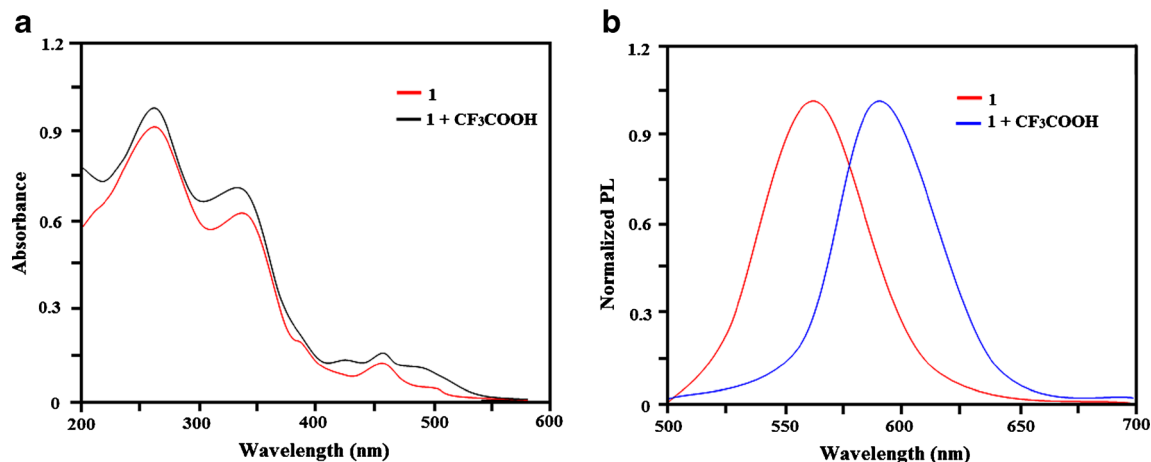


**Fig. 8** Absorption and photoluminescence spectra of **1** in  $\text{CH}_3\text{CN}$  solution before and after addition of  $\text{CF}_3\text{COOH}$

the addition of  $F^-$ , the absorption bands of **1** at 263 nm gradually decrease and three new bands appeared at 308, 442, and 478 nm with three distinct isobestic points at 286, 370 and 425 nm. This result indicates strong ground state interactions between **1** and the fluoride anion, and a dramatic color change from green to brown observed (Fig. 6). Similar results were observed for complex salts **2**, **3** and **4** upon addition of the fluoride anion (Fig. 5). The emission spectra titrations of **1–4** with anions were also measured and the emission of the four complex salts is quenched upon addition of  $F^-$ . Moreover, similar changes in absorption and emission spectra of complex salts were also observed when other anions  $CH_3COO^-$  and  $H_2PO_4^-$  were added. The quenching implied strong interaction between the complex salts and these anions. The binding constant values ( $K$ ) for complex salts calculated from fluorescence data are displayed in Table 3. The binding constant values ( $K$ ) of **1** for  $F^-$ ,  $CH_3COO^-$ , and  $H_2PO_4^-$  were  $6.98 \times 10^4$ ,  $2.63 \times 10^4$ , and  $4.92 \times 10^3 M^{-1}$ , respectively (Table 3). Complex salt **1** can be used as a selective chemosensor for fluoride anion. For comparison purpose the effect of anion with complex salt **5** was also carried out. No obvious change in UV–vis absorption and emission spectra was observed for **5** upon addition of  $F^-$ . Therefore it was concluded that the interaction of NH of phenanthroline ligands (**1–4**) with anion is responsible for the significant optical variations. In addition, the intramolecular N–H–F–P hydrogen bonds existing in these complex salts can also enhance the acidity of N–H, increasing the deprotonation trend [49–54]. The influence of fluoride anions on the electrochemical properties of **1–4** was also analysed. After the addition of fluoride anions, no evident change was observed for the reduction wave (Fig. 7) indicating that the interaction of anions with imidazole N–H does not change the LUMO energy level. However, the addition of fluoride anion causes obvious variation of the oxidation wave. Upon addition of fluoride anions, the oxidation potential attributed to the iridium center and Ir–C  $\sigma$ -bond orbitals was shifted positively and a new irreversible oxidation wave appeared at more negative potential. The irreversible oxidation wave at 0.59 V is assigned to the oxidation of the imidazolyl group after deprotonation. The mechanism of fluorescence quenching in the presence of  $F^-$ ,  $CH_3COO^-$ , and  $H_2PO_4^-$  is somewhat ambiguous. The deprotonation process results in a greater degree of distortion between its excited and ground state surfaces and increases the probability of radiationless transitions. In addition, there is also a probability of a photoinduced electron transfer (PET) process from the lone pair on the imidazolyl group after deprotonation, which quenches the emission of complex salts.

#### Effect of Proton on Tuning Photophysical and Electrochemical Properties

Significant changes in UV–vis absorption and emission spectra were observed when  $CF_3COOH$  was added into the

$CH_3CN$  solutions of **1–4**. Figure 8 gives the variation of photophysical properties of **1** upon addition of  $CF_3COOH$ . The emission wavelength of **1** was red-shifted and the emission color changed from green to red (Fig. 6). Similar results were observed for complex salts **2–4** upon addition of  $CF_3COOH$ . Protonation increasing the overall degree of delocalization of the imidazolyl and phenyl units and hence causing a large stabilization which is responsible for the obvious red shift of emission wavelength. In addition, the electrochemical properties of **1–4** were also investigated upon addition of  $CF_3COOH$ . The reduction waves of **1–4** assigned to the reduction of the N^N ligands were markedly shifted positively. So, protonation of the N^N ligand can reduce the energy levels of the LUMO more significantly and decrease the energy of the triplet excited state.

#### Conclusions

In conclusion, we have synthesized a series of new cationic iridium(III) complex salts containing different imidazo[4,5-*f*]-[1, 10]phenanthroline derivatives. The influence of anions and proton on the photophysical and electrochemical properties were studied in detail. After the addition of  $CF_3COOH$ , the emission wavelength of the complex salts were significantly red-shifted and the emission colors changed from green to red. The emission of the complex salts was quenched completely and the solution colors of changed from green to brown by the addition of anions  $F^-$ ,  $CH_3COO^-$  and  $H_2PO_4^-$ . The calculated binding constant values confirmed that all the newly synthesized complex salts are ideal phosphorescent chemosensor for  $F^-$ . This anion-sensing results gives a new route in designing a series of new phosphorescent probes based on iridium(III) complexes by simply modifying the structures of the ligands and also help in the exploration for new applications of iridium(III) complexes as chemosensors.

**Acknowledgments** One of the authors Prof. J. Jayabharathi is thankful to DST [No. SR/S1/IC-73/2010], DRDO (NRB-213/MAT/10-11) and CSIR (NO 3732/NS-EMRII) for providing funds to this research study.

#### References

- Baldo MA, O'Brien DF, You Y, Shoustikov A, Sibley S, Thompson ME, Forrest SR (1998) Highly efficient phosphorescent emission from organic electroluminescent devices. *Nature* 395:151
- Chen Z, Bian Z, Huang C (2010) Functional Ir(III) complexes and their applications. *Adv Mater* 22:1534
- Coppo PE, Plummer A, Cola LD (2004) Tuning iridium(III) phenylpyridine complexes in the “almost blue” region. *Chem Commun* 1774
- Chang CJ, Yang CH, Chen K, Chi Y, Shu CF, Ho M-L, Yeh YS, Chou PT (2007) Color tuning associated with heteroleptic cyclometalated Ir(III) complexes: influence of the ancillary ligand. *Dalton Trans* 1881

- Liang B, Wang L, Xu YH, Shi HH, Cao Y (2007) High-efficiency red phosphorescent iridium dendrimers with charge-transporting dendrons: synthesis and electroluminescent properties. *Adv Funct Mater* 17:3580–3589
- Gong X, Robinson MR, Ostrowski JC, Moses D, Bazan GC (2002) High-efficiency polymer-based electrophosphorescent devices. *J Adv Mater* 14:581–585
- Bera RN, Cumpstey N, Burn PL, Samuel IW (2007) Highly branched phosphorescent dendrimers for efficient solution-processed organic light-emitting diodes. *Adv Funct Mater* 17:1149–1152
- Xu ZW, Li Y, Ma XM, Gao XD, Tian H (2008) Synthesis and properties of iridium complexes based 1,3,4-oxadiazoles derivatives. *Tetrahedron* 64:1860–1867
- Lin ZH, Zhao YG, Duan CY, Zhang BG, Bai ZP (2006) A highly selective chromo- and fluorogenic dual responding fluoride sensor: naked-eye detection of F<sup>-</sup> ion in natural water via a test paper. *Dalton Trans* 3678–3684
- Brinas R, Troxler T, Hochstrasser RM, Vinogradov SA (2005) Phosphorescent oxygen sensor with dendritic protection and two-photon absorbing antenna. *J Am Chem Soc* 127:11851–11862
- Tang WS, Lu XX, Wong KMC, Yam VWW (2005) Synthesis, photophysics and binding studies of Pt(II) alkynyl terpyridine complexes with crown ether pendant. Potential luminescent sensors for metal ions. *J Mater Chem* 15:2714–2720
- Neve F, Deda ML, Crispini A, Bellusci A, Puntoriero F, Campagna S (2004) Anisometric cyclometalated palladium (II) and platinum (II) complexes. Structural and photophysical studies. *Organometallics* 23:5856–5863
- Liu SJ, Zhao Q, Chen RF, Deng Y, Fan QL, Li FY, Wang LH, Huang CH, Huang W (2006) Pi-conjugated chelating polymers with charged iridium complexes in the backbones: synthesis, characterization, energy transfer, and electrochemical properties. *Chem Eur J* 12:4351–4361
- Gao R, Ho DG, Hernandez B, Selke M, Murphy D, Djurovich PI, Thompson ME (2002) Bis-cyclometalated Ir(III) complexes as efficient singlet oxygen sensitizers. *J Am Chem Soc* 124:14828–14829
- Huynh L, Wang Z, Yang J, Stoeva V, Lough A, Manners I, Winnik MA (2005) Evaluation of phosphorescent rhenium and iridium complexes in polythionylphosphazene films for oxygen sensor applications. *Chem Mater* 17:4765–4773
- Zhao Q, Cao TY, Li F, Li XH, Jing H, Yi T, Huang CH (2007) A highly selective and multisignaling optical-electrochemical sensor for Hg<sup>2+</sup> based on a phosphorescent iridium(III) complex. *Organometallics* 26:2077–2081
- Beer PD, Gale PA (2001) Anion recognition and sensing: the state of the art and future perspectives. *Angew Chem Int Ed* 40:486–516
- (2003) *Coord Chem Rev* 240(1 and 2) (Special Issues on anion receptors)
- Suksai C, Tuntulani T (2003) Chromogenic anion sensors. *Chem Soc Rev* 32:192–202
- Bondy CR, Gale PA, Loeb SJ (2004) Metal organic analogs of calix[4]arene based anion receptors. Arranging urea hydrogen-bond acceptors to selectively bind chloride and sulfate ions. *J Am Chem Soc* 126:5030–5031
- Wallace KJ, Belcher WJ, Syed KF, Seed JW (2003) Slow anion exchange, conformational equilibria and fluorescent sensing in Venus flytrap aminopyridinium-based anion hosts. *J Am Chem Soc* 125:9699–9715
- Best MD, Tobey SL, Anslyn EV (2003) Abiotic guanidinium containing receptors for anionic species. *Coord Chem Rev* 240:3–15
- Choi K, Hamilton AD (2003) Macrocyclic anion receptors based on directed hydrogen bonding interactions. *Coord Chem Rev* 240:101–110
- Haj-Zaroubi M, Mitzel NW, Schmidtchen FP (2002) The rational design of anion host compounds: an exercise in subtle energetics. *Angew Chem Int Ed* 41:104–107
- Liu ZQ, Shi M, Li FY, Fang Q, Chen ZH, Yi T, Huang CH (2005) Highly selective two-photon chemosensors for fluoride derived from organic boranes. *Org Lett* 7:5481–5484
- Zhou ZG, Xiao SZ, Xu J, Liu ZQ, Shi M, Li FY, Yi T, Huang CH (2006) Modulation of the photochromic property in an organoboron-based diarylethene by a fluoride ion. *Org Lett* 8:3911–3914
- Zhou ZG, Yang H, Shi M, Xiao SZ, Li FY, Yi T, Huang CH (2007) Photochromic organoboron-based dithienylcyclopentene modulated by fluoride and mercuric(II) ions. *ChemPhysChem* 8:1289–1292
- Goodall W, Williams JAG (2000) Iridium(III) bis-terpyridine complexes incorporating pendent *N*-methylpyridinium groups: luminescent sensors for chloride ions. *J Chem Soc Dalton Trans* 2893–2896
- Zhao Q, Liu S, Shi M, Li F, Jing H, Yi T, Huang C (2007) Tuning photophysical and electrochemical properties of cationic iridium(III) complex salts with imidazolyl substituents by proton and anions. *Organometallics* 26:5922–5930
- Liu T, Zhang HX, Zhou X, Zheng QC, Xia BH, Pan QJ (2008) Mechanism of Ir(ppy)<sub>2</sub>(N N')(+) (N N'=2-phenyl-1H-imidazo[4,5-f][1,10]phenanthroline) sensor for F<sup>-</sup>, CF<sub>3</sub>COOH, and CH<sub>3</sub>COO<sup>-</sup>: density functional theory and time-dependent density functional theory studies. *J Phys Chem A* 112(36):8254–8262
- Jayabharathi J, Thanikachalam V, Sathishkumar R, Jayamoorthy K (2013) Physico-chemical studies of fused phenanthrimidazole derivative as sensitive NLO material. *Spectrochim Acta A* 101:249–253
- Nonoyama K (1974) Benzo(*h*)quinolin-10-yl-N iridium(III) complexes. *Bull Chem Soc Jpn* 47:467–468
- Lamansky S, Djurovich P, Murphy D, Abdel-Razzaq F, Kwong R, Tsyba I, Bortz M, Mmui B, Bau R, Thompson ME (2001) Synthesis and characterization of phosphorescent cyclometalated iridium complexes. *Inorg Chem* 40:1704–1711
- Mi BX, Wang PF, Liu MW, Kwong HL, Wong NB, Lee CS, Lee ST (2003) Thermally stable hole-transporting materials for organic light-emitting diode: an isoindole derivative. *Chem Mater* 15:3148–3151
- DePriest J, Zheng GY, Goswami N, Eichhorn DM, Woods C, Rillema DP (2000) Structure, physical, and photophysical properties of platinum (II) complexes containing bidentate aromatic and bis(diphenylphosphino)methane as ligands. *Inorg Chem* 39:1955–1963
- Jayabharathi J, Thanikachalam V, Srinivasan N, Venkatesh Perumal M (2011) Physicochemical studies of green phosphorescent light-emitting materials from cyclometalated heteroleptic iridium(III) complexes. *Spectrochim Acta A* 79:338–347
- Saravanan K, Srinivasan N, Thanikachalam V, Jayabharathi J (2011) Synthesis and photophysics of some novel imidazole derivatives used as sensitive fluorescent chemosensors. *J Fluoresc* 21:65–80
- Jayabharathi J, Thanikachalam V, Saravanan K (2009) Effect of substituents on the photoluminescence performance of Ir(III) complexes: synthesis, electrochemistry and photophysical properties. *J Photochem Photobiol A* 208:13–20
- Brooks K, Babayan Y, Lamansky S, Djurovich PI, Tsyba I, Bau R, Thompson ME (2002) Synthesis and characterization of phosphorescent cyclometalated platinum complexes. *Inorg Chem* 41:3055–3066
- Jayabharathi J, Thanikachalam V, Srinivasan N, Jayamoorthy K, Venkatesh Perumal M (2011) An intramolecular charge transfer fluorescent probe: synthesis, structure and selective fluorescent sensing of Cu<sup>+2</sup>. *J Fluoresc* 21:1813–1823
- Okada S, Okinaka K, Iwawaki H, Furugori M, Hashimoto M, Mukaide T, Kamatani J, Igawa S, Tsuboyama A, Takiguchi T, Ueno K (2005) Substituent effects of iridium complexes for highly efficient red OLEDs. *Dalton Trans* 9:1583–1590
- Schmid B, Graces FO, Watts RJ (1994) *Inorg Chem* 33:9
- Lamansky S, Djurovich PI, Murphy D, Abdel-Razzaq F, Lee HE, Forrest SR, Thompson ME (2001) Highly phosphorescent bis-cyclometalated iridium complexes synthesis, photophysical characterization, and use in organic light emitting diodes. *J Am Chem Soc* 123:4304–4312

44. Tamayo AB, Alleyne BD, Djurovich PI, Lamansky S, Tsyba I, Ho NN, Bau R, Thompson ME (2003) Synthesis and characterization of facial and meridional tris cyclometalated iridium(III) complexes. *J Am Chem Soc* 125:7377
45. Colombo MG, Udel HUG (1993) Synthesis and high-resolution optical spectroscopy of bis(2-(2-thienyl)pyridinato-C3, N')(2,2'-bipyridine)iridium(III). *Inorg Chem* 32:3081–3087
46. Colombo MG, Brunold TC, Riedener T, Güdel HU, Füllörtsch M, Burgi HB (1994) Facial tris cyclometalated  $Rh^{3+}$  and  $Ir^{3+}$  complexes: their synthesis, structure, and optical spectroscopic properties. *Inorg Chem* 33:545–550
47. Spellane P, Watts RJ, Vogler A (1993) Luminescence characterizations of cyclometalated rhenium(1) carbonyl complexes. *Inorg Chem* 32:5633–5636
48. Calogero G, Giuffrida G, Serroni S, Ricevuto V, Campagna S (1995) Absorption spectra, luminescence properties, and electrochemical behavior of cyclometalated iridium (III) and rhodium (III) complexes with a bis (pyridyl) triazole ligand. *Inorg Chem* 34:541–545
49. Gunnlaugsson T, Kruger PE, Jensen P, Pfeffer FM, Hussey GM (2003) Simple naphthalimide based anion sensors: deprotonation induced colour changes and  $CO_2$  fixation. *Tetrahedron Lett* 44: 8909–8913
50. Lee JY, Cho EJ, Mukamel S, Nam KC (2004) Efficient fluoride-selective fluorescent host: experiment and theory. *J Org Chem* 69: 943–950
51. Boiocchi M, Boca LD, Esteban-Gómez D, Fabbrizzi L, Licchelli M, Monzani E (2004) Nature of urea- fluoride interaction: incipient and definitive proton transfer. *J Am Chem Soc* 126:16507–16514
52. Amendola V, Boiocchi M, Fabbrizzi L, Palchetti A (2005) Anion receptors containing -NH binding sites: hydrogen-bonding formation or neat proton transfer. *Chem Eur J* 11:120–127
53. Boiocchi M, Boca LD, Esteban-Gómez D, Fabbrizzi L, Licchelli M, Monzani E (2005) Anion induced urea deprotonation. *Chem Eur J* 11:3097–3104
54. Gomez DE, Fabbrizzi L, Licchelli M, Monzani E (2005) Urea vs. thiourea in anion recognition. *Org Biomol Chem* 3:1495–1500